# Fast Modal Identification, Monitoring, and Visualization for Large-Scale Power Systems using Dynamic Mode Decomposition

Saurav Mohapatra
PowerWorld Corporation
Champaign, IL, USA
saurav@powerworld.com

Thomas J. Overbye
Department of Electrical and Computer Engineering
University of Illinois
Urbana, IL, USA
overbye@illinois.edu

***Abstract*—Dynamic Mode Decomposition (DMD) is a relatively new method for simultaneous modal analysis of multiple time-series signals. In this paper, DMD is successfully applied towards transmission-level power system data in an implementation that is able to run quickly. Since power systems are considered as non-linear and time-varying, modal identification is capable of monitoring the evolution of large-scale power system dynamics by providing a breakdown of the constituent oscillation frequencies and damping ratios, and their respective amplitudes. DMD is an efficient algorithm for both off-line and on-line processing of large volumes of time-series measurements, which can enable spatio-temporal analyses, improve situational awareness, and could even contribute towards control strategies. This paper applies DMD on a set of simulated measurements consisting of both frequency and voltage magnitude data. The key advantage of this implementation is its relatively fast computation; for example, it is able to process a $7$ s time-window, consisting of $3392$ signals with $211$ time points, in $0.185$ s. Automated processing of transient contingency results, and on-line mode tracking are two proposed applications.**

***Index Terms*—Modal identification, power system dynamics, transient stability, situational awareness, and visualization.**

## I. Introduction

Electric power systems are never truly in steady state due to continuous small load fluctuations. However, control devices are able to keep a system's operating point within a narrow band during these small variations in load, which can be referred to as a pseudo-steady state. Sometimes planned/unplanned events can cause large perturbations that might result in more oscillatory behavior, and eventually lead to a new pseudo-steady state. These dynamics are known to occur in the Transient Stability time frame. Knowledge about the dominant oscillation modes characterizes a system's temporal evolution and stability attributes ([1]).

Modal identification from measurements provides information about oscillation frequencies and damping ratios, and their respective amplitudes and phase. Identifying poorly damped modes can help in tuning control strategies for better stabilization ([1]). In today's highly interconnected electric grid, a disturbance originating from one part of the system can affect the entire system. Moreover, the presence of low-inertia and intermittent renewable generation units can also result in greater deviation from a desired operating point. These practical concerns in stability and control motivate the need for closer to real-time spatio-temporal awareness of a system's dynamic trajectories ([2]), which can be aided with accurate estimation of modes and mode shapes from measurements.

Modal estimation can be performed using any type of measurements (ambient, ring-down, or probing), and there are methods which are better suited for each data type (explained in Section II). Ring-down analysis methods, such as Prony ([3]), Matrix Pencil (MPM) ([4]), Eigensystem Realization (ERA) ([5]) and Variable Projection (VPM) ([5]), have been applied to power system measurements. However in this paper, a method known as Dynamic Mode Decomposition (DMD) is implemented for ring-down analysis, which originated from the Fluid Dynamics field in $2008$ ([6], [7]). First applied to power systems in [8], this work showed that DMD can be substantially faster than Prony.

This paper focuses on the use of DMD for short time-interval modal identification for a wide-area interconnected power system to exhibit DMD's strength in accommodating a large set of measurement channels, while still being computationally fast. This paper also shows that if different types of measurement channels are augmented with each other, it can help strengthen the precision of calculations, and hence allow a smaller time-window to be used. Before describing DMD, the modal analysis problem is briefly described in Section II, along with references to relevant past and current work that have been utilized in the industry. Next, the DMD algorithm is summarized in Section III, followed by Section IV, which presents an application of DMD. Results, and spatio-temporal visualization are shown, which conveys the wealth of information extracted via DMD, so as to inspire its use by power system operators and in smart grid analytics. A discussion of DMD's fast computational speed is presented, and some applications are proposed.

This work was supported by the National Science Foundation (award number 1128325).

## II. Problem Statement and Literature Review

If a dynamic model of a power system is available, modal analysis could be done through the linearization of differential-algebraic equations (DAEs), representing a system and operating point of interest ([9]). Apart from calculating modes, the participation factors (based on the eigenvectors of the linearized state matrix) reveal the impact of each state on each mode (and vice-versa). Some modes are affected by several states, and other modes are only impacted by a few states. Since different states can be associated with different geographic locations, modes are said to be local or inter-area depending on their geographic extent. Local and inter-area modes have also been observed in measurement data.

However, from a practical perspective, model-based modal analysis is challenging due to the time-varying nature of power systems. Approximate values can be obtained from calculations using planning models that usually run in an off-line manner. To reduce the dependency on models, and as an alternate approach, most measurement-driven modal analysis schemes calculate values of $\sigma_i$ (damping), $\omega_i$ (angular frequency), $c_i$ (amplitude) and $\phi_i$ (phase), and ultimately seek to reconstruct a signal as a sum of damped sinusoids,

$$\hat{y}(t) = \sum_{i=1}^{I} c_i e^{\sigma_i t} \cos(\omega_i t + \phi_i), \tag{1}$$

given the measurement signal $y(t)$. Typically this is done for a duration of time, $0 \leq t \leq T$. Methods like Prony, MPM, and ERA assume that the signal is an output of a linear time-invariant system, while VPM in [10] does not require this assumption, because non-linear basis functions can be chosen as part of VPM. Nevertheless, a signal can be expressed in terms of eigenvalues, $\lambda_i = \sigma_i \pm \mathrm{j}\omega_i$. Similar to equation (1), a sum of damped sinusoids can be represented in discrete-time,

$$\hat{y}[n] = \sum_{j=1}^{J} d_j \left(\mu_j\right)^n, \tag{2}$$

for $n \in [0, N]$, $n \in \mathbb{Z}$, $d_j \in \mathbb{C}$, $\mu_j \in \mathbb{C}$, and where the sample number, $n$, and the sampling interval, $\Delta t$ are related by the equation $n = t/\Delta t$. Typically, measurements are recorded with evenly-spaced samples, and therefore, the reconstructed signals in equations (1) and (2) are practically equivalent. The number of summation terms in equations (1) and (2) are $I$ and $J$ respectively. They satisfy the relationship $J - I =$ Number of complex conjugate eigenvalue pairs, because terms arising from complex conjugate pairs of the discrete-time eigenvalues ($\mu_j$ and $\overline{\mu}_j$) map to a single term in the continuous time summation in equation (1), i.e.,

$$d_j(\mu_j)^n + \overline{d}_j(\overline{\mu}_j)^n = c_i e^{\sigma_i n \Delta t} \cos(\omega_i n \Delta t + \phi_i). \tag{3}$$

Many methods calculate $\lambda_i$ by finding $\mu_j$ from a discrete-time series, and require the time-series signal(s) to be uniformly sampled. If there are missing measurements, or signals are being combined from two or more sources, then interpolation and re-sampling are needed. Some implementations of these methods have incorporated an optional pre-processing step for removing the initial/final/mean value of the signal and/or removing linear or quadratic trends ([11], [12]). Some methods also incorporate the filtering of noise, and this also has proven useful in improving accuracy in some cases.

Methods like Prony ([13]), MPM ([14], [15]), and ERA ([16]) use a two-step procedure to first estimate the eigenvalues and then estimate the mode shapes ([17], [18]). The industry has continued to seek alternatives so as to monitor system dynamics more closely, and for maintaining good operating points ([19]). Work has been done using a system identification approach ([20]), and also with ambient measurements ([21], [22]). Methods like stepwise-regression ([23]) have also been formulated as an add-on to Prony analysis. Newer methods have been designed to better understand the error bounds in mode estimation ([24]), and also provide an understanding of the transfer-function representation of power systems ([25]). Some of these measurement-based methods have also been tested with measurements taken during probing conditions. The concept of modal energy trending has recently been used, which utilizes a combination of frequency-domain and Singular Value Decomposition (SVD) methods ([26], [27]).

Similar to some other methods, DMD also consists of two steps, which first estimates the modal frequency and damping, and then their respective amplitude and phase. One by-product of DMD's first step is a mapping between underlying dynamics and measurements, which is strategically used in simplifying the second optimization step (not done in Prony, MPM, and ERA). An assumption in DMD is an approximately constant linear mapping between consecutive measurement samples during one time-window. Despite this assumption, there is firm theoretical foundation for applying DMD towards analyzing nonlinear dynamics ([28]) in power systems. DMD is considered as a numerical algorithm for finding the modes of the infinite-dimensional linear Koopman operator, which is defined for any nonlinear system ([29]). Koopman modes are closed related to the system modes, and hence DMD modes accurately represent the system modes ([30]). Arnoldi schemes in [31] and [32] are related to DMD via a similarity transformation ([7]), and in theory can also estimate Koopman modes; however, they are less robust than DMD, and hence not suitable for practical implementations. These Arnoldi schemes have been applied towards power systems ([33], [34]), but DMD has only been recently applied in [8].

## III. Dynamic Mode Decomposition

DMD is inherently an ensemble spectral analysis technique, and therefore modal identification is done using a multi-signal approach. As shall be shown, a key advantage in the application of DMD to power systems is its computational speed. DMD is known to be able to extract coherent structures in either simulated or real measurements (even with noise) and associate them to single oscillation frequencies ([30]), i.e. modes. DMD requires uniformly sampled measurements;

for this, $N+1$ samples are gathered for a time-window of interest, $\mathcal{T}_{[t-T,t]}$, with a sample interval of $\Delta t$ and duration of $T$. Therefore, $T = N\Delta t$. Given $M$ signals, each with $N+1$ samples, these values are cast into a matrix,

$$\mathbf{Y} = \begin{bmatrix} \mathbf{y}_0 & \mathbf{y}_1 & \dots & \mathbf{y}_n & \dots & \mathbf{y}_N \end{bmatrix} \in \mathbb{C}^{M\times(N+1)}. \quad (4)$$

For generality, and from the perspective of the DMD algorithm, these measurements could be complex valued. Next, $\mathbf{Y}$ is separated into two matrices:
$\mathbf{Y}_0 = \begin{bmatrix} \mathbf{y}_0 & \dots & \mathbf{y}_{N-1} \end{bmatrix}$, and $\mathbf{Y}_1 = \begin{bmatrix} \mathbf{y}_1 & \dots & \mathbf{y}_N \end{bmatrix}$. By assuming an approximately constant linear mapping, $\mathbf{A}$, consecutive measurement samples can be related by,

$$\mathbf{y}_n \approx \mathbf{A}\mathbf{y}_{n-1}, \qquad \text{for} \qquad n = [1, N], n \in \mathbb{Z}, \quad (5)$$

for a time duration, $T$, and hence $\mathbf{Y}_1$ and $\mathbf{Y}_0$ are related by,

$$\mathbf{Y}_1 = \mathbf{A}\mathbf{Y}_0 + \boldsymbol{\rho}\boldsymbol{\eta}_N^{\mathrm{T}}, \quad (6)$$

where $\boldsymbol{\rho}\boldsymbol{\eta}_N^{\mathrm{T}}$ is the residual error. The work in [29] and [30] elaborate on the orthogonality of $\boldsymbol{\rho}$ to the measurement space spanned by the columns of $\mathbf{Y}_0$. Based on the projection theorem, this is the smallest possible error ([29]).

In what follows, the key steps of the DMD algorithm are described. For a detailed discussion on the theory of DMD, linear algebra manipulations and the estimation of DMD modes for nonlinear systems, please refer to articles [7], [30], [28], and [35]. DMD consists of two parts – (i) estimation of discrete-time eigenvalues, and (ii) estimation of complex amplitudes of respective modes. Algorithm 1 summarizes the steps of DMD. In part I, $R$ discrete-time eigenvalues are calculated, followed by the calculation of the corresponding $R$ complex amplitudes in part II. These values are encapsulated in $\boldsymbol{\mu}$ and $\boldsymbol{\alpha}$ respectively. These discrete-time eigenvalues can be conveniently converted to continuous-time eigenvalues: $\sigma_i + \mathrm{j}\omega_i = \lambda_i = \ln(\mu_j)/\Delta t = (\ln|\mu_j| + \mathrm{j}\angle\mu_j)/\Delta t$ for $-\pi < \angle\mu_j \leq \pi$. Additionally, matrix $\mathbf{E}$ with columns $\mathbf{e}_r$, and matrix $\mathbf{U}$ with rows $\mathbf{u}_m$, are by-products that help reconstruct measurement $m$ at time point $n$. It is given by a summation of the individual modes weighted by their respective amplitudes, then mapped to $R$ hidden states by the eigenvectors of $\tilde{\mathbf{A}}$, and then mapped via the appropriate left singular vector to the $m^{\text{th}}$ signal. Similar to (2), each reconstructed signal is,

$$\hat{y}_m[n] = \mathbf{u}_m^{\mathrm{T}} \sum_{r=1}^{R} \mathbf{e}_r \alpha_r \mu_r^n = \sum_{r=1}^{R} \hat{y}_{(m,r)}[n], \quad (7a)$$

$$\text{where} \quad \hat{y}_{(m,r)}[n] = \mathbf{u}_m^{\mathrm{T}} \mathbf{e}_r \alpha_r \mu_r^n, \quad (7b)$$

is the contribution of each mode. This allows for efficient spatio-temporal slicing and dicing of an array of measurement signals. Since DMD is inherently an ensemble spectral analysis technique, modal analysis is carried out using a multi-signal approach. Although not detailed in this paper, DMD utilizes a least-squares optimization approach ([35]). Hence, the optimal values of $\boldsymbol{\mu}$ and $\boldsymbol{\alpha}$ are the closed-form expressions shown in Algorithm 1 that help minimize the least-squares residue between all the measurement and reconstructed signals.

**Algorithm 1** Dynamic Mode Decomposition

**Data**: $\mathbf{Y} = \begin{bmatrix} \mathbf{y}_0 & \mathbf{y}_1 & \dots & \mathbf{y}_N \end{bmatrix} \in \mathbb{C}^{M\times(N+1)}$
**Result**: $\mathbf{U}$, $\mathbf{E}$, $\boldsymbol{\alpha}$, and $\boldsymbol{\mu}$

1: $\mathbf{Y}_0 \leftarrow \begin{bmatrix} \mathbf{y}_0 & \dots & \mathbf{y}_{N-1} \end{bmatrix}$, and $\mathbf{Y}_1 \leftarrow \begin{bmatrix} \mathbf{y}_1 & \dots & \mathbf{y}_N \end{bmatrix}$

**Part I** Estimation of discrete-time eigenvalues
2: $\mathbf{U}\boldsymbol{\Sigma}\mathbf{V}^{\mathrm{H}} \leftarrow$ economy size SVD of $\mathbf{Y}_0$, and retain $R$ non-zero singular values
3: $\tilde{\mathbf{A}} \leftarrow \mathbf{U}^{\mathrm{H}}\mathbf{Y}_1\mathbf{V}\boldsymbol{\Sigma}^{-1}$
4: $\mathbf{E}\mathbf{D}_\mu\mathbf{E}^{-1} \leftarrow$ eigen decomposition of $\tilde{\mathbf{A}}$
5: $\boldsymbol{\mu} \leftarrow \mathrm{diag}(\mathbf{D}_\mu)$

**Part II** Estimation of complex amplitudes
6: $\boldsymbol{\alpha} \leftarrow \mathbf{E}^{-1}\boldsymbol{\Sigma}\mathbf{V}^{\mathrm{H}}_{[1,*]}$

Notes:
(i) $\mathbf{U}, \mathbf{V} \in \mathbb{C}^{M\times R}$, $\mathbf{U}^{\mathrm{H}}\mathbf{U} = \mathbf{I}$, and $\mathbf{V}^{\mathrm{H}}\mathbf{V} = \mathbf{I}$
(ii) $\tilde{\mathbf{A}} \in \mathbb{C}^{R\times R}$

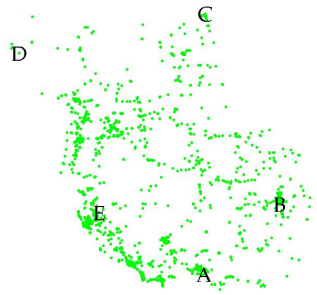


Figure 1: Spatial visualization of 1696 measurement locations from an interconnected power grid, with 5 locations labeled

## IV. Application of DMD

In the past, small sets of transient contingencies were simulated and analyzed. With advances in the modeling of power system dynamics, focus has been shifting towards running longer simulations and many more transient contingencies. Distributed computing has also enabled the running multiple simulations in parallel. The industry seems to be quickly approaching a point where running a large set of transient contingencies is no longer a bottleneck, but interpreting their simulations results is. Power system engineers also face the task of deciphering all the data that is available from sensors such as Phasor Measurement Units (PMUs), Frequency Disturbance Recorders (FDRs) ([36]), and Digital Fault Recorders (DFRs). Modal analysis via DMD fits this need.

### A. Synthetic Measurement Data, via Simulation

To emulate data from actual PMUs, a transient stability simulation of an industry-grade dynamic model of a large-scale interconnected power grid was used to collect synthetic

frequency measurements at 1696 high-voltage locations spanning a wide-area (but a small portion of the total buses in the system). All load models were augmented with a Gaussian load noise model (7% standard deviation) with a low pass filter ($\tau = 0.5$ s) to capture the effect of random load fluctuations, so as to mimic the aggregate effect of load variations that occur in an actual power system. In this simulation a large perturbation was introduced through the loss of a large generation unit at $t = 1$ s, and transient behavior was recorded for 30 s. Figure 2 shows the spread of frequencies at 1696 locations during the fault, with one signal highlighted. Frequency and voltage magnitude measurements were gathered at 30 samples/second, which is equivalent to 6.21 Mbits/s, if they were to be available as a stream. With reference to DAE models for transient stability analysis, and participation factor analysis [9], voltage magnitude and frequency quantities could be thought of as different outputs of the same underlying dynamic system. Hence, time-series voltage magnitude and frequency signals are expected to contain the same modal constituents, but with different coefficients.

For generality, this set of measurements is treated as a streaming data source input. The DMD algorithm was implemented in a software code, which accepts this data stream. A trailing $T$-second time-window concept was utilized, such that the output data reflects the modal content in the prior $T$ seconds of measurements. This time-window was advanced with a step-size, $t_{\text{step}}$. The idea of sliding time-windows is common for speech recognition, where the signal content is time-varying, and has also been utilized in power systems literature ([37]). The power system measurements being processed in this example originate from a non-linear time-varying system. Therefore, frequency-domain information is expected to vary with time. The choice of the window length, $T$ is application specific ([38]) as it presents a trade-off between resolutions in time-domain or frequency-domain. For power system measurements, this value of $T$ can be tuned, based on historical knowledge of the approximate system eigenvalues. In the example being presented here, $T = 7$ s, and $t_{\text{step}} = \frac{1}{30}$ s were chosen. However, these are suggested values, which could be modified based on the application or preference. This significant overlap between consecutive time-windows and the fast solution of DMD is hoped to allow for continual short-interval mode tracking.

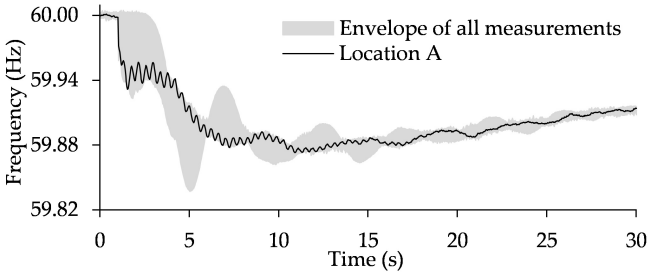


Figure 2: Frequency measurements from 1696 locations

### B. Results from One Time-Window

As discussed in Section III, DMD is capable of analyzing multiple signals simultaneously. In this example, all 3392 measurement signals (frequency and voltage magnitude) were analyzed concurrently for each time-window. The dominant 3 modes for the time-window $\mathcal{T}_{[4.0,11.0]}$ are summarized in Table I. Similar to the observations in [8], DMD is able to perform well and provides meaningful results. For this time-window and others (and with other data sets), DMD consistently yielded very small least squares normalized residues on the order of $10^{-10}$ or lower. In this particular time-window, modes 1 and 2 have low damping ratios, while the damping ratio for mode 3 is significantly greater. Only mode 3 can be considered to be well damped.

### C. Tracking the Dominant Mode using a Moving Window

The DMD analysis is repeated using a moving window implementation on the simulated streaming voltage magnitude and frequency measurements. Using a trailing time-window of $T = 7$ s, and $t_{\text{step}} = \frac{1}{30}$ s. Once again, these are user-defined. The choice of $t_{\text{step}} = \frac{1}{30}$ s is the smallest possible value, and is intentional so that variation in the dominant ac mode can be studied. Figure 3 shows the variation of the dominant ac mode with time, i.e., the points at $t = 11.2$ s are calculated based on a trailing time window $\mathcal{T}_{[4.2,11.2]}$. Since $t_{\text{step}} = \frac{1}{30}$ s, there are 31 data points in this plot. This can be compared to the dominant ac mode in Table I, which is about 0.19886 Hz, and shows small variations over time, as expected due to system non-linearity and DMD estimation error from using a finite time-window. Experiments were also conducted by using only frequency or only voltage magnitude data, and the observed variations were found to an order of magnitude higher. In the case of the dominant mode, it was relatively easy to track visually, or a nearest-neighbor type of algorithm could be implemented for automated tracking. Nevertheless, the variation in modes is relatively smooth. Note, the above discussion was on the dominant oscillation mode in the entire system. However during dynamic behavior, the dominant mode in one part of the system might differ from another location in the same system. In other words, the amplitude (or the energy content) of a particular mode can vary based on the location, the fault, and the operating point.

### D. Spatio-Temporal Results from Frequency and Voltage Magnitude Data

Since both frequency and voltage magnitude data have been utilized for this analysis, each location is associated with two

TABLE I: Modal analysis of frequency and voltage magnitude measurements during time-window $\mathcal{T}_{[4.0,11.0]}$.

| Modes | Oscillation frequency (Hz) | Damping ratio |
|---|---|---|
| 1 | 0.19886 | 0.074679 |
| 2 | 0.31007 | 0.027697 |
| 3 | 0.40178 | 0.46923 |

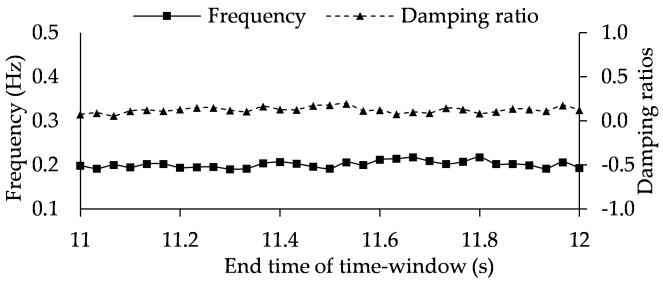


Figure 3: Variation in oscillation frequency and damping ratio of the dominant ac mode, using a trailing time window, $T = 7$ s, and $t_{\text{step}} = \frac{1}{30}$ s, and input data at 30 samples/s. Standard deviation of oscillation frequency: 0.00764 Hz. Standard deviation of damping ratio: 0.0324.

types of signals. From a geographic viewpoint, one could imagine two layers of data associated with the footprint of the system being studied. Modal estimation with DMD has been done simultaneously for all these signals, which expresses each layer of measurement data as a location-wise sum of several modes. If there are $R$ modes, then that corresponds to $R$ mode layers for each layer of measurement data. Table II shows the temporal evolution of two such mode layers, which corresponds to modes 1 and 2 from Table I. The area shown corresponds to that from Figure 1, and is able to capture wide-area effects of individual modes. For confidentiality reasons the absolute values of amplitudes have been excluded; however, the snapshots show modal amplitudes varying in time and space. These holistic contour animations provide a more intuitive approach than looking at numerical values of modal amplitudes and phase shifts.

The series of snapshots shown in Table II is from an animation of the mode amplitudes during time-window $\mathcal{T}_{[4.0,11.0]}$. Recall from Equation 7b that the amplitude of $r^{\text{th}}$ mode present in $m^{\text{th}}$ signal is $\mathbf{u}_m^{\mathrm{T}}\mathbf{e}_r\alpha_r$. As seen here, the spatio-temporal variation of each mode can be observed. The spatial variation of mode amplitudes is gradual in the frequency layer. From a system-level view, there is a phase difference between the two modes, and this is expected due to the presence of many dynamic components in the system. The contour animations associated with the voltage magnitude layer are more interesting, as they exhibit the inter-area manifestation of modes, but also show localized effects. The spatial variation in modes is more pronounced in the voltage layer, which ties in well with the idea that voltage dynamics are often in localized clusters.

From the perspective of the frequency layer, mode 1 is seen to divide the system into two areas, and mode 2 divides the system into 3 areas. These are usually known as inter-area modes. However for each of these modes, the corresponding voltage layer exhibits different spatial areas. So if an inter-area mode is observed between a particular set of areas in the frequency layer, the areas observed in the voltage layer can be different. This indicates that the amplitude and the phase of a particular mode can be different between the frequency and voltage magnitude signals measured at the same location.

Modal-content-based criteria could be used to automatically monitor all the signals being analyzed by DMD. This can enable selective saving of transient stability results that violate said criteria, and hence reduce data storage needs. Similar

TABLE II: Spatial visualization of mode amplitudes during time-window $\mathcal{T}_{[4.0,11.0]}$ (modes 1 and 2 are listed in Table I).

| Mode | Signal | t = 4.0 s | t = 4.1 s | t = 4.3 s | t = 4.6 s | t = 5.1 s | t = 5.9 s | t = 7.2 s | t = 9.3 s |
|---|---|---|---|---|---|---|---|---|---|
| 1 | $f$ | | | | | | | | |
| | $\lvert V\rvert$ | | | | | | | | |
| 2 | $f$ | | | | | | | | |
| | $\lvert V\rvert$ | | | | | | | | |

Relative Scale: negative — zero — positive

criteria could be used in an on-line setting to intelligently sieve out the most relevant modes or signals, which can then be used in control rooms. Animation (as illustrated in Table II) could be created and destroyed on-the-fly to aid in system-wide situational awareness of dynamic trajectories.

## V. Discussion and Summary

The software code was also evaluated by varying the number of measurement signals and the number of samples in each time-window. CPU timing tests with the current code showed that the DMD computation time scaled at about $\mathcal{O}(N^3)$ with respect to the number of samples in the time-window of interest, and at about $\mathcal{O}(M)$ with respect to the number of measurement channels, similar to as published in [39]. This is even true when $M \gg N$. Figure 4 shows a plot of this trend. Given the computational complexity and absolute time needed to solve, DMD is efficient for modal identification, especially in being able to accommodate a large number of measurement channels. Results from the previous sections show that DMD is able to track the dominant oscillation mode during a transient contingency.

DMD is inherently an ensemble analysis method, and it is computationally cheap to incorporate a large number of measurement channels. Some publications suggest using a subset of the measurement channels that have been pre-selected based on historical information or heuristics for fast modal estimation using methods such as Prony, MPM, or ERA. However, in the case of DMD, using many measurement channels is actually useful as it helps with noisy data, and also mitigates data quality issues (as shown in [39]). If one of many signals being used is "bad", then the effect on modal estimation would be minimal, as opposed to, if data is corrupted in one out of a small set of pre-selected measurement channels. Another reason for using multiple signals is to be able to process them in parallel and detect instability in a small number of signals during their initial unstable growth.

As stated in [39], having measurement channels that capture a full phase cycle is helpful for DMD's performance. Although not shown in this paper, augmenting frequency with voltage magnitude signals did help in reducing the rapid change in modal estimation, as compared to only using frequency data. Using a longer time window could have also helped in averaging out the modes and reducing the fluctuations further. For example, in [8], time-windows of about $20-40$ s are utilized. However, using longer time window in DMD is computationally more expensive ($\mathcal{O}(N^3)$) than using extra measurement signals ($\mathcal{O}(M)$). So instead of using longer time-windows, multiple measurement channels of different data types should be used in DMD analyses. The result is better precision, even though a smaller time-window is used, and fast modal estimation. By using a smaller time-window, the time-varying estimates of a dominant mode are less influenced by averaging over a longer time-window. Also, using multiple channels can help maintain the quality of modal estimates; therefore, using smaller time-windows would be sufficient.

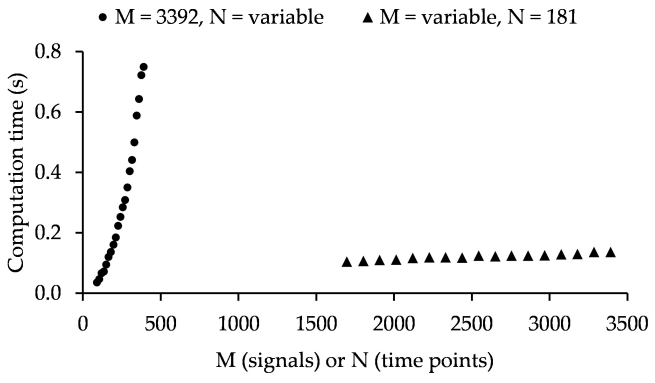


Figure 4: Computation times using a 2.7 GHz dual core processor vs. variations in number of signals, $M$, and number of time points, $N$.

PMUs and PMU-like devices are being installed in large numbers, and infrastructure is being commissioned to collect and store this data. Since the computational cost associated with DMD is low, it may be of interest to process multiple channels of measurements at data concentrator locations or control centers, and then broadcast holistic measures such as oscillation frequencies, damping ratios, and respective amplitudes. In this way, the circulation of raw measurement data would be reduced, and wide-area closed loop control schemes could be designed by incorporating the above-mentioned holistic metrics. Although the algorithm presented in this paper assumes a central processing style, it is possible to implement DMD in a distributed and incremental manner, which will be explored in future research.

As an example, DMD is able to process $3392$ measurement channels with $211$ time points in $0.185$ s. This implies that DMD can be repeated with new time points as soon as the previous DMD calculation is completed. Once a particular time-window of measurement channels has been gathered at a data concentrator, the algorithmic latency of a moving window DMD analysis would be $0.185$ s in an on-line setting. The efficiency of DMD can also aid in fast off-line processing of results from multiple transient contingency simulations. Intelligent ways of adaptively down-sampling and/or varying the length of the time-window are topics of practical interest that could make DMD more precise and robust.

There are other tools which automatically calculate and monitor the modal content of a collection of power system measurements. DMD is hoped to be a good addition to the list of such tools, and to be especially useful for simultaneous analysis of thousands of measurement channels. DMD might also prove useful in the case of a series of transient contingencies, or possibly a cascading failure scenario. Since the "ring-down" duration will be relatively short for each consecutive fault, DMD could be able to accommodate short-time interval data (from many channels), and still give good modal estimates in a fast computation time. With DMD, it is no longer computationally prohibitive to do modal analysis for a large set of a measurement data. In conclusion, this paper exhibits DMD's strength in accommodating a large set of measurement

channels, while using different types of measurement channels to strengthen the precision of calculations. This allow a smaller time-window to be used, and hence results in low latency calculations.

## REFERENCES


[1] P. Kundur, *Power System Stability and Control*. McGraw-Hill Education, 1994.

[2] J. Hauer, E. Martinez, A. R. Messina, and J. Sanchez-Gasca, "Identification of Electromechanical Modes in Power Systems," Tech. Rep., 2012.

[3] J. Hauer, C. Demeure, and L. Scharf, "Initial results in Prony analysis of power system response signals," *IEEE Transactions on Power Systems*, vol. 5, no. 1, pp. 80–89, 1990.

[4] Y. Hua and T. Sarkar, "Matrix pencil method for estimating parameters of exponentially damped/undamped sinusoids in noise," *IEEE Transactions on Acoustics, Speech, and Signal Processing*, vol. 38, no. 5, pp. 814–824, may 1990.

[5] I. Kamwa, R. Grondin, E. Dickinson, and S. Fortin, "A minimal realization approach to reduced-order modelling and modal analysis for power system response signals," *IEEE Transactions on Power Systems*, vol. 8, no. 3, pp. 1020–1029, 1993.

[6] P. Schmid and J. Sesterhenn, "Dynamic mode decomposition of numerical and experimental data," *Bulletin of the American Physical Society*, vol. 53, nov 2008.

[7] P. J. Schmid, L. Li, M. P. Juniper, and O. Pust, "Applications of the dynamic mode decomposition," *Theoretical and Computational Fluid Dynamics*, vol. 25, no. 1-4, pp. 249–259, aug 2010.

[8] E. Barocio, B. C. Pal, N. F. Thornhill, and A. R. Messina, "A dynamic mode decomposition framework for global power system oscillation analysis," *IEEE Transactions on Power Systems*, 2014.

[9] G. Rogers, *Power System Oscillations*. Kluwer Academic Publishers, 2000.

[10] A. R. Borden and B. C. Lesieutre, "Variable projection method for power system modal identification," *IEEE Transactions on Power Systems*, vol. 29, no. 6, pp. 2613–2620, nov 2014.

[11] N. Zhou, D. Trudnowski, J. W. Pierre, S. Sarawgi, and N. Bhatt, "An algorithm for removing trends from power-system oscillation data," in *2008 IEEE Power and Energy Society General Meeting - Conversion and Delivery of Electrical Energy in the 21st Century*. IEEE, jul 2008, pp. 1–7.

[12] A. R. Borden, B. C. Lesieutre, and J. Gronquist, "Power system modal analysis tool developed for industry use," in *2013 North American Power Symposium (NAPS)*. IEEE, sep 2013, pp. 1–6.

[13] G. Prony, *Multiexponential Fitting Algorithm. Numerical Analysis*. New York: McGraw-Hill, 1974.

[14] V. Jain, "Filter analysis by use of pencil of functions: Part I," *IEEE Transactions on Circuits and Systems*, vol. 21, no. 5, pp. 574–579, sep 1974.

[15] ——, "Filter analysis by use of pencil of functions: Part II," *IEEE Transactions on Circuits and Systems*, vol. 21, no. 5, pp. 580–583, sep 1974.

[16] J. N. Juang and R. S. Pappa, "An eigensystem realization algorithm for modal parameter identification and model reduction," *Journal of guidance, control, and dynamics*, vol. 8, no. 5, pp. 620–627, oct 1985.

[17] G. H. Golub and V. Pereyra, "The differentiation of pseudo-inverses and nonlinear least squares problems whose variables separate," *SIAM Journal on Numerical Analysis*, vol. 10, no. 2, pp. 413–432, apr 1973.

[18] G. Golub and V. Pereyra, "Separable nonlinear least squares: the variable projection method and its applications," *Inverse Problems*, vol. 19, no. 2, pp. R1–R26, apr 2003.

[19] Z. Huang, N. Zhou, F. Tuffner, and Y. Chen, *MANGO: Modal Analysis for Grid Operation: a Method for Damping Improvement Through Operating Point Adjustment*, 2010.

[20] J. Pierre, D. Trudnowski, M. Donnelly, N. Zhou, F. Tuffner, and L. Dosiek, "Overview of system identification for power systems from measured responses," in *System Identification*, vol. 16, no. 1, jul 2012, pp. 989–1000.

[21] J. Pierre, D. Trudnowski, and M. Donnelly, "Initial results in electromechanical mode identification from ambient data," *IEEE Transactions on Power Systems*, vol. 12, no. 3, pp. 1245–1251, 1997.

[22] D. Trudnowski, J. Pierre, and W. Mittelstadt, "Electromechanical mode online estimation using regularized robust RLS methods," *IEEE Transactions on Power Systems*, vol. 23, no. 4, pp. 1670–1680, nov 2008.

[23] N. Zhou, J. W. Pierre, and D. Trudnowski, "A stepwise regression method for estimating dominant electromechanical modes," *IEEE Transactions on Power Systems*, vol. 27, no. 2, pp. 1051–1059, may 2012.

[24] L. Dosiek, J. W. Pierre, and J. Follum, "A recursive maximum likelihood estimator for the online estimation of electromechanical modes with error bounds," *IEEE Transactions on Power Systems*, vol. 28, no. 1, pp. 441–451, feb 2013.

[25] L. Dosiek and J. W. Pierre, "Estimating electromechanical modes and mode shapes using the multichannel ARMAX model," *IEEE Transactions on Power Systems*, vol. 28, no. 2, pp. 1950–1959, may 2013.

[26] Z. Tashman and V. M. Venkatasubramanian, "Modal energy trending for ringdown analysis in power systems using synchrophasors," in *2014 47th Hawaii International Conference on System Sciences*. IEEE, jan 2014, pp. 2475–2482.

[27] E. Rezaei, L. Zhang, and V. Venkatasubramanian, "Self-correction strategies for frequency domain ringdown analysis," in *2015 48th Hawaii International Conference on System Sciences*. IEEE, 2015, pp. 2690–2699.

[28] J. H. Tu, C. W. Rowley, D. M. Luchtenburg, S. L. Brunton, and J. N. Kutz, "On dynamic mode decomposition: Theory and applications," *Journal of Computational Dynamics*, vol. 1, no. 2, pp. 391–421, nov 2014.

[29] C. W. ROWLEY, I. MEZIĆ, S. BAGHERI, P. SCHLATTER, and D. S. HENNINGSON, "Spectral analysis of nonlinear flows," *Journal of Fluid Mechanics*, vol. 641, p. 115, nov 2009.

[30] P. J. SCHMID, "Dynamic mode decomposition of numerical and experimental data," *Journal of Fluid Mechanics*, vol. 656, pp. 5–28, jul 2010.

[31] L. N. Trefethen, D. Bau, and III, *Numerical Linear Algebra*. SIAM, 1997.

[32] A. Greenbaum, *Iterative Methods for Solving Linear Systems*. SIAM, 1997.

[33] Y. Susuki and I. Mezic, "Nonlinear Koopman modes and power system stability assessment without models," *IEEE Transactions on Power Systems*, vol. 29, no. 2, pp. 899–907, mar 2014.

[34] F. Raak, Y. Susuki, T. Hikihara, H. R. Chamorro, and M. Ghandhari, "Partitioning power grids via nonlinear Koopman Mode Analysis," in *ISGT 2014*. IEEE, feb 2014, pp. 1–5.

[35] M. R. Jovanović, P. J. Schmid, and J. W. Nichols, "Sparsity-promoting dynamic mode decomposition," *Physics of Fluids*, vol. 26, no. 2, p. 024103, feb 2014.

[36] Z. Zhong, C. Xu, B. Billian, L. Zhang, S.-J. Tsai, R. Conners, V. Centeno, A. Phadke, and Y. Liu, "Power system frequency monitoring network (FNET) implementation," *IEEE Transactions on Power Systems*, vol. 20, no. 4, pp. 1914–1921, nov 2005.

[37] V. Venkatasubramanian, "Oscillation monitoring from ambient PMU measurements by frequency domain decomposition," in *2008 IEEE International Symposium on Circuits and Systems*. IEEE, may 2008, pp. 2821–2824.

[38] A. V. Oppenheim and R. W. Schafer, *Discrete-Time Signal Processing*. Pearson Education, 2011.

[39] D. Duke, J. Soria, and D. Honnery, "An error analysis of the dynamic mode decomposition," *Experiments in Fluids*, vol. 52, no. 2, pp. 529–542, dec 2011.